

Quantitative Vitreous Fluorophotometry Applying a Mathematical Model of the Eye

Henrik Lund-Andersen,* Bent Krogsaa,* Morten la Cour,* and Jesper Larsen†

A slit-lamp fluorophotometric method is presented that permits calculation of a blood-retinal barrier permeability to fluorescein (P) and a diffusion coefficient for fluorescein in the vitreous body (D). The calculations are performed by relating the time course of the free—not protein bound—fluorescein concentration in the bloodstream with the fluorescein concentration profile in the vitreous body. The combination is performed automatically on a computer by applying a simplified mathematical model of the eye. P refers to the area of the barrier of the model eye. In a group of six normal persons, the mean P was $(1.1 \pm 0.4) \times 10^{-7}$ cm/sec (mean \pm SD), while in six diabetic patients with background retinopathy and macular edema the mean P was $(7.1 \pm 3.8) \times 10^{-7}$ cm/sec. The mean D was $(7.4 \pm 3.4) \times 10^{-6}$ cm²/sec in the normal group and $(9.6 \pm 2.0) \times 10^{-6}$ cm²/sec in diabetic patients, corresponding as a first approximation to free diffusion in water. Model calculations show that knowing the fluorescein concentration in the bloodstream is considerably significant for the calculation of the permeability, contributing factors up to 50%. For the low-permeation situation, subtraction of the preinjection scan contributes a factor of 50% for both permeability and diffusion coefficient. The exact placement in the vitreous body of the concentration profile, by applying a formalism that transforms slit-lamp movement to intraocular distance, contributes a factor of 20% on the diffusion coefficient. The permeability obtained with the model can be calculated as the ratio between area of vitreous and plasma fluorescein concentration curves within 20%.

Active transport of fluorescein across the blood-retinal barrier in the direction of vitreous to blood does not seem to be significant within the first 2 hr after fluorescein injection. *Invest Ophthalmol Vis Sci* 26:698-710, 1985

During the last 8 years, vitreous fluorophotometry has been used to quantitate the permeability properties of the blood-retinal barrier to fluorescein.

The method, originally introduced by Cunha-Vaz and co-workers,^{1,2} has been based upon intravenous (IV) injection of a standard dose of fluorescein, which usually after 60 min was followed by a slit-lamp photometric determination of the fluorescein concentration in the vitreous body. The magnitude of the concentration in the posterior part of the vitreous body has been used as a measurement of the barrier permeability. However, as it has been pointed out, it is important to incorporate the fluorescein concentration in the plasma in the calculation of the perme-

ability of the barrier³⁻¹³ and to include more than the concentration of fluorescein in a single point of the vitreous body in the calculations. An analysis of the fluorescein concentration profile in the vitreous body can, furthermore, provide qualitative information of the diffusion properties in the vitreous body.¹⁴ Quantitative evaluation of this factor has previously been reported for the anterior vitreous³ and recently for the posterior part of the vitreous body, based upon first principles.¹³

The present article presents a more complete method for the calculation of a blood-retinal barrier permeability to fluorescein and a diffusion coefficient for fluorescein in the posterior part of the vitreous body. The method is based upon simultaneous determinations of the fluorescein concentration in plasma and in vitreous body. These data are combined on a computer by applying a simplified mathematical model of the eye to give a fluorescein permeability of the barrier and a diffusion coefficient for fluorescein in the vitreous body. The method, which is based on a series of studies of 165 human examinations, is presented here in detail. The individual clinical studies will be presented elsewhere in separate articles. The mathematical model has been described previously,¹⁰

From University Eye Clinic,* Rigshospitalet, and Math-Tech Institute,† Rosenstandsvej, Copenhagen, Denmark.

Supported by The Danish Medical Research Council, The Novo Foundation, The National League of Diabetes, Minister Erna Hamiltons Grant, The Committee for Prevention of Blindness, and The Danish Organisation for Fight against Eye Diseases and Blindness.

Submitted for publication: January 20, 1984.

Reprint requests: Henrik Lund-Andersen, MD, PhD, University Eye Clinic, Rigshospitalet E2061, Blegdamsvej 9, DK-2100 Copenhagen, Ø, Denmark.

while preliminary reports of the entire method presented herein have been given elsewhere.^{11,12,15,16}

Materials and Methods

Fluorophotometric Equipment

Slit lamp: The slit lamp is a Rodenstock 2001 mounted with oculars (700-10 Gamma Scientific; San Diego, CA) which in their focal point contain a 450 μm fiber optic probe picking up light from the slit-lamp focal plane as described by Cunha-Vaz¹ and by Krogsaa et al.¹⁷ In the focal plane, the slit is 1 mm high and 0.1 mm wide. The angle between slit and symmetry axis of the biomicroscope is 11.4° and the angle between symmetry axis and ocular is 5.6° . The light source of the slit lamp is a 450 W xenon arc lamp connected with the slit lamp by a fiber optic cable. This cable is interrupted by a light chopper (Rofin 7500; Rofin, England), which chops the light with a frequency of 432 Hz. The intensity of the blue light in the slit is 5 mW/cm^2 , as determined by a fluxmeter (Hewlett Packard type 8330 A). The filters used are a blue (SWP 495) and yellow (LWP 515) interference filter (Optical Laboratory; Lyngby, Denmark), with transmission characteristics as shown in Figure 1.

Amplification and registration equipment: The light from the optic probe in the ocular is passed to a photomultiplier (initially a Gamma Scientific Model D-46 but now a PR-1400 RF, Products for Research Inc.; Danvers, MA) operated at room conditions. The photomultiplier is directly connected with an amplifier triggered from the chopper (Lock-in, Model 128 A, Princeton Applied Research; Princeton, NJ). This system increases the sensitivity of the equipment by a factor of seven. The lock-in amplifier is connected to the Y-axis of a X-Y recorder (Philips PM 8041; Eindhoven, Netherlands). The sagittal movement of the slit lamp is transduced to the X-axis of the recorder by a precision potentiometer. A mechanical device connected to the potentiometer secures that the movement of the slit lamp occurs in the sagittal plane. A foot switch allows an indication to be made on the X-axis in all desired positions of the slit-lamp focal plane and thereby also the ocular fiber optic probe in relation to the ocular structures, which are in focus when the focal plane is moved from retina to cornea. The X-Y recorder is coupled in parallel to a microcomputer (SPC/1, Danish Data Electronics; Copenhagen, Denmark) via an analog digital converter for on-line registration of the X-Y and foot switch signals. The microcomputer is connected to a central computer (Control Data Corporation Cyber, 170; St. Paul, MN) provided with a graphic terminal (Tektronix 4051; Beaverton, OR). The entire set-up is schematically shown in Figure 2.

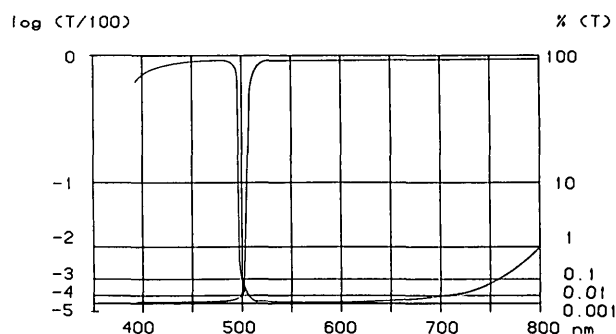


Fig. 1. Transmission characteristics of the blue excitation filter and yellow barrier filter. The transmission (T) on ordinate is shown as a function of wavelength (nm) on abscissa. The ordinate shows (left) $\log (T/100)$ and (right) % of unrestricted transmission. Both filters are interference filters obtained from Optical Laboratory Lyngby, Denmark (see Materials and Methods).

Sensitivity and spatial resolution of the equipment:

The sensitivity of the equipment defined as the concentration required to yield a signal twice as high as the background noise was $2.5 \times 10^{-9} \text{ g/ml}$. A cross-section of the volume of measurement—the optical diamond^{18,19}—is constituted by a parallelogram measuring $(0.48 \times 2.16) \text{ mm}$ with a diagonal of 2.64 mm. The spatial resolution was tested in a double compartment cuvette (Fig. 3). This showed that at a distance of more than 1.2 mm from the wall that separates two compartments, the signal in one compartment is influenced less than 2.3% by the signal from the other compartment.

Although the optical diamond, as calculated from an analysis of the optics of the slit-lamp equipment, has the same geometry in these in vitro experiments

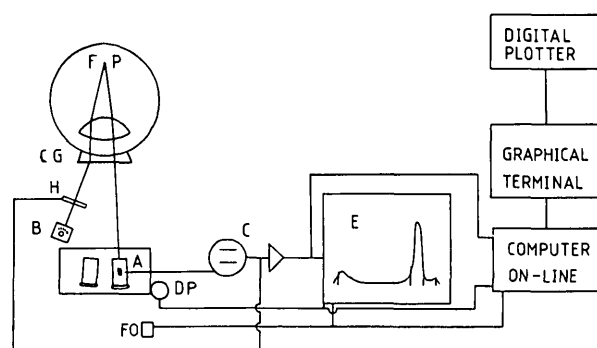


Fig. 2. Schematic presentation of the slit lamp and computer equipment. A: ocular with fiber optic probe; B: Xenon light source; C: photomultiplier and lock-in amplifier; DP: potentiometer transducing slit-lamp movement to recorder and computer; E: X-Y recorder; FO: foot switch for indications of the focal plane in the eye; CG: is contact glass; H: light chopper in connection with the lock-in amplifier; FP: the focal plane of the slit lamp. The X-Y recorder is connected in parallel with a computer system consisting of a smaller one for on line registration of data and a larger for data calculation. Curves are presented on a graphical terminal and digital plotter.

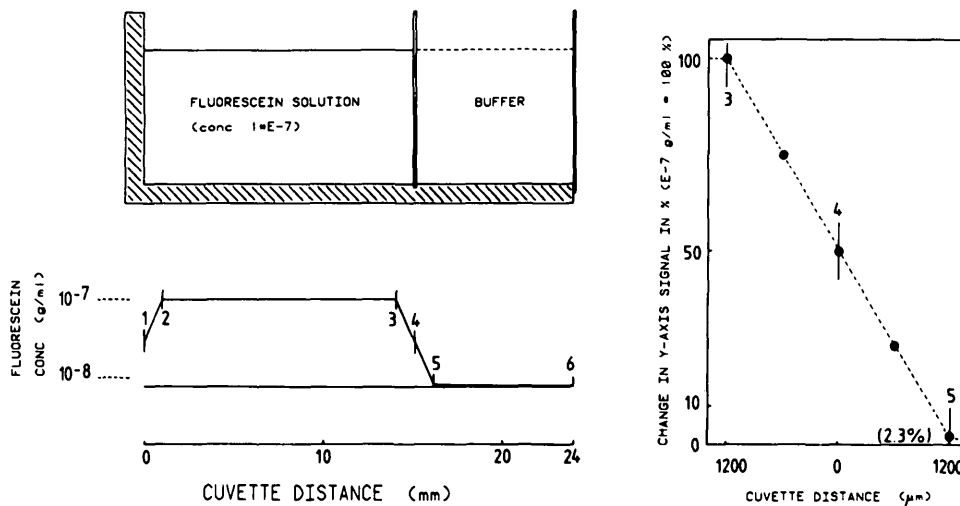


Fig. 3. Illustration of the spatial resolution of the slit-lamp equipment. *Top left*, the concentration is measured in a double cuvette separated by a glass wall of 100 μm . The concentration of fluorescein in the left chamber is 1×10^{-7} g/ml while it is zero in the right chamber. *Bottom left*, the concentration profile through the cuvette is shown. The marker points 1-6 represent the following positions of the slit lamp focal plane and optic fiber: (1) posterior wall of the cuvette in focus; (2) optic fiber free of the blue slit image on the posterior

wall of the cuvette; (3) optic fiber at the posterior surface of the wall between the two chambers; (4) wall between the two chambers in the middle of the optic fiber; (5) optic fiber at the anterior surface of the wall between the two chambers; (6) optic fiber at the anterior wall of the cuvette. *Right*, the profile at the separation between the two chambers is magnified. It appears that the signal has diminished to 2.3% of the maximal signal 1200 μm from the wall which separates the two chambers. This is a maximal value, since the background signal originating from the buffer solution alone is not subtracted from the values given in the figure.

as in the eye,¹⁷ it should be stressed that the ideal measurements of the optical resolution should be performed *in vivo*.

The Fluorophotometric Examination

Fluorescein administration and analysis in blood: Fluorescein (14 mg/kg body weight) was injected in an antecubital vein over a 60-sec period. From a cannula in an antecubital vein in the other arm, blood samples were obtained before, and 5, 15, 30, 60, and 120 min after injection. After centrifugation plasma was analyzed for total as well as free (not protein-bound) fluorescein concentration, the latter by ultrafiltration, as described in detail elsewhere.^{6,7}

Briefly, the analysis is performed in the following way: Blood is collected in heparinized test tubes. After centrifugation plasma is ultrafiltered using the Amicon MPS-1 system (Amicon Corporation; Danvers, MA). Initially, Millipore Ultra Free disposable filters were used, giving the same results as the Amicon filters. The total fluorescein concentration is determined after sufficient dilution of plasma. As a control of the method and an estimation of the free fluorescein concentration in the bolus during its first passage through the ocular circulation, fluorescein is added to plasma samples obtained before injection of fluorescein; these samples were analyzed in the same way as the other plasma samples. The concentration of total fluorescein in these test samples is 5×10^{-6} g/ml, 5×10^{-5} g/ml, and 3×10^{-4} g/ml, the latter corresponding to the assumed concentration in

the bolus. The free fraction constitutes approximately 15% for all the concentration ranges.⁷

The bolus concentration: The concentration of fluorescein in the ocular arterial, capillary, and venous system during the fluorescein injection is unknown (the bolus concentration), but it can be estimated according to the following reasoning. The fluorescein solution (1×10^{-1} g/ml) is injected over a 1-min period. It is assumed that the cardiac output is 5 l/min; hematocrit, 43%; and recirculation and extraction in pulmonary circulation is neglected. A person of 70 kg will receive 9.8 ml fluorescein over the 1-min period, and the total plasma fluorescein concentration in the bolus will accordingly be

$$\frac{10^{-1} \times 9.8}{5000 \times 0.57} = 3.4 \times 10^{-4} \text{ g/ml.}$$

Assuming an unbound fluorescein concentration of 15% at this concentration,⁷ the concentration in the bolus during the 1 min of injection will be 5×10^{-5} g/ml.

Fluorophotometry: The present article is based on experience obtained over a 3-year period in which 165 examinations were performed. Two typical examinations, one with low leakage (normal person) and one with high leakage (diabetic patient), are shown in the article. The examination is performed after the eye is anaesthetized with oxybuprocaine (0.4%) and the pupil dilated with metaoxidrin (10%) and 0.5% tropicamide. A Goldmann contact lens (Haag-Streit AG; Liebefeld, Switzerland) with specifications given elsewhere¹⁷ is used. An axial fluores-

cence scan is made before injection of fluorescein and 30, 60, and 120 min after injection. The scan is obtained in the following way: First the macula is focused. The slit lamp and its focal plane is then moved manually toward the examiner through the vitreous body, the lens, and the anterior chamber with a speed of less than 2 mm/sec, which secures that the amplification system, which operates with a time constant of 0.3 sec, is able to follow the slit-lamp movement. A time constant of 0.1 sec gave the same results. However, the noise was then too high for the low-permeation situation, and 0.3 sec was chosen for all measurements. A feedback system signals if the speed is higher than 2 mm/sec.¹⁸ The movement of the slit lamp is stopped and the foot switch activated marker mechanism is activated at the following positions (Fig. 7A) position 1, the foveola is in focus; position 2, the fiber optic probe is free of the blue image on the retina (this is approximately 1.5 mm from the retina); positions 3 and 6, the fiber optic probe is located at the posterior and anterior surface of the lens, respectively; positions 4 and 5, posterior and anterior lens surface, respectively, in the middle of the optic fiber; position 7, optic fiber at the posterior corneal surface; and position 8, posterior corneal surface in the middle of the optic fiber. Scans are made two to three times at each time indicated (before, 30, 60, and 120 min after injection of fluorescein). P and D are calculated as the means of the P and D values obtained for each scan. The reproducibility of the determination was acceptable, since the standard deviation (SD) of the determinations obtained at the same time was less than 25% of the mean. The apparatus is calibrated and automatically adjusted with a 1×10^{-7} g/ml fluorescein phosphate buffer solution before each set of measurements.

Informed consent was obtained from the persons examined after the nature of the procedures had been explained fully.

Calculation of a Blood-Retinal Barrier Permeability and a Diffusion Coefficient in the Vitreous Body

The calculation of permeability (P) and diffusion coefficient (D) is performed by linking the concentration course of free fluorescein in the plasma with the concentration profile in the vitreous body. This linkage is performed by the application of a simplified model of the eye. The model that will be described in more detail below is coupled on a large computer (see Larsen et al¹⁰). However, before transmission of data to the large computer, three procedures are performed on the small computer (SPC/1), where data are collected on line: (1) the X-axis is transformed to real

intraocular distances; (2) the fluorescence signal obtained before injection is subtracted from the signal obtained after injection; and (3) the amount of data is reduced.

Transformation of the X-axis to intraocular distance: The movement of the slit lamp is, as mentioned, transduced to the X-axis by a potentiometer. By knowing the amplification of recorder and potentiometer, a movement on the X-axis can be transformed to movement of the slit lamp. The slit lamp movement, however, cannot be transformed directly to intraocular distances. Due to the refraction of light in the compound optical system, the movement of the slit-lamp focal plane is different from the movement of the slit lamp itself.^{15,17,18,20} With the knowledge of the ratio between the two movements, the X-axis movement of the pen on the recorder can be transformed to intraocular distances according to the equation:

$$X_e = X_r \times F \times M \quad (1)$$

where X_e is intraocular distance; X_r , distance on recorder; F, the ratio (movement of focal plane in the eye/movement of slit lamp); and M, the amplification of recorder and potentiometer, which in the present set up is 1:12.1.

As shown by Krogsaa et al.¹⁷ for a standard Gullstrand eye, $F = 1.45$ for movement through the anterior chamber, $F = 1.64$ for movement through the lens, and $F = 1.44$ for movement through the vitreous body. By application of these values, the length of the individual parts of the eye can be calculated from a curve shown in Figure 7A, and the axial length of the eye is calculated as the sum of these three segments.²⁰ The radius of the eye is calculated as one half of the axial length. The factor F varies through the individual ocular compartments as shown in Figure 4. This variation is of significance for the location of the concentration profile in the vitreous body. For that purpose the radius of the eye is divided in segments of 0.5 mm, and the value of F for each segment is used during the vitreal location of the concentration profile according to equation (1).

Correction for preinjection value: The autofluorescence signal, which is obtained before injection of fluorescein, is converted to intraocular fluorescence signal by the same procedure as described above. The ordinate value of corresponding intraocular positions of the preinjection curve is subtracted automatically from the actual concentration profile obtained.

Data reduction: In order to reduce the amount of data before transmission to the central computer data are reduced so that only Y-values for every 200- μ m intraocular distance are transmitted. Only data from

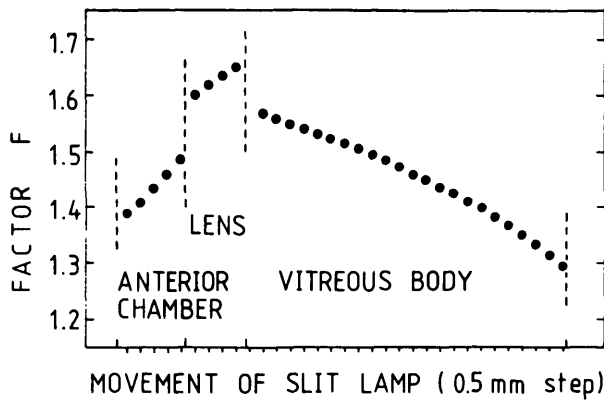


Fig. 4. Ratio (F) between intraocular movement of the slit-lamp focal plane and movement of slit lamp. F is calculated by an analysis of the optical pathway as schematically illustrated in Figure 2 and described in more detail elsewhere.¹⁷ F is calculated for every 0.5-mm movement of the slit lamp. It appears that F is different for the three segments of the eye (anterior chamber, and vitreous body) and varies within the individual compartments.

marker point 2 to the center of the eye are transmitted to the computer and used for further analysis.

Together with the transmission of the concentration profile, the time course of the free fluorescein concentration in the plasma is also transmitted to the central computer.

The Simplified Model of the Eye and its Mathematical Formalism

The simplified model: In order to calculate a permeability of the blood-retinal barrier and a diffusion coefficient in the vitreous body a simplified model of the eye was developed, as schematically shown in Figure 5. It appears from Figure 5 that the blood-retinal barrier is symbolized by a single membrane surrounding a homogeneous gel, ie, the vitreous

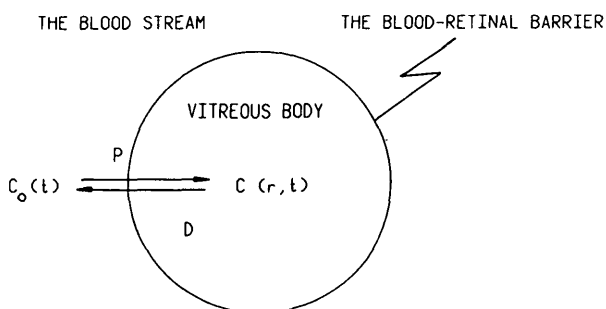


Fig. 5. Simplified model of the eye used for the computerized calculation of a blood-retinal barrier permeability and vitreous body diffusion coefficient for the substance fluorescein. $C_0(t)$: concentration of free (not protein-bound) fluorescein in plasma at time (t); $C(r,t)$: concentration of fluorescein in the vitreous body at time (t) and at the position (r) from the center of the eye; P: permeability of the blood-retinal barrier, symbolized by a single spherical shell; D: diffusion coefficient in the vitreous body.

body, and separating the vitreous body from the bloodstream. Fluorescein is assumed to penetrate the barrier with a constant permeability (P) and to move in the vitreous body only by diffusion with a constant diffusion coefficient (D). The time-dependent plasma fluorescein concentration is given by $C_0(t)$ and the concentration in the vitreous body dependent upon time (t) and distance (r) from the center of the eye is given by $C(r,t)$.

The mathematical formalism: The formulation of the mathematical formalism and the solution of the equations which describe the combination of the model parameters are given in detail elsewhere.¹⁰ Below, the main equations are given for the description of the mathematical model:

$$c(r, t) = \int_0^t c_0(t-s) \cdot F(r, s; a, D, P) ds, \quad (2)$$

where

$$F(r, s; a, D, P) = \frac{aP}{r\sqrt{D}} \times \left[G\left(\frac{a-r}{2\sqrt{D}}, s; k\right) - G\left(\frac{a+r}{2\sqrt{D}}, s; k\right) \right]. \quad (3)$$

In (3) G is given by

$$G(x, s; k) = e^{-x^2/4s}/\sqrt{\pi s} - k \cdot e^{k(x+k \cdot s)} \operatorname{erfc}(k\sqrt{s} + x/2\sqrt{s}), \quad (4)$$

where $k = (P/\sqrt{D}) - (\sqrt{D}/a)$ and erfc is the complementary error function. Radius (a) of the eye is determined experimentally (compare with Materials and Methods).

The equations are programmed on the central computer. P and D are calculated from a set of experimental data by minimizing

$$S = \sum_{i=1}^N w_i [c_m(r_i, t) - c(r_i, t)]^2, \quad (5)$$

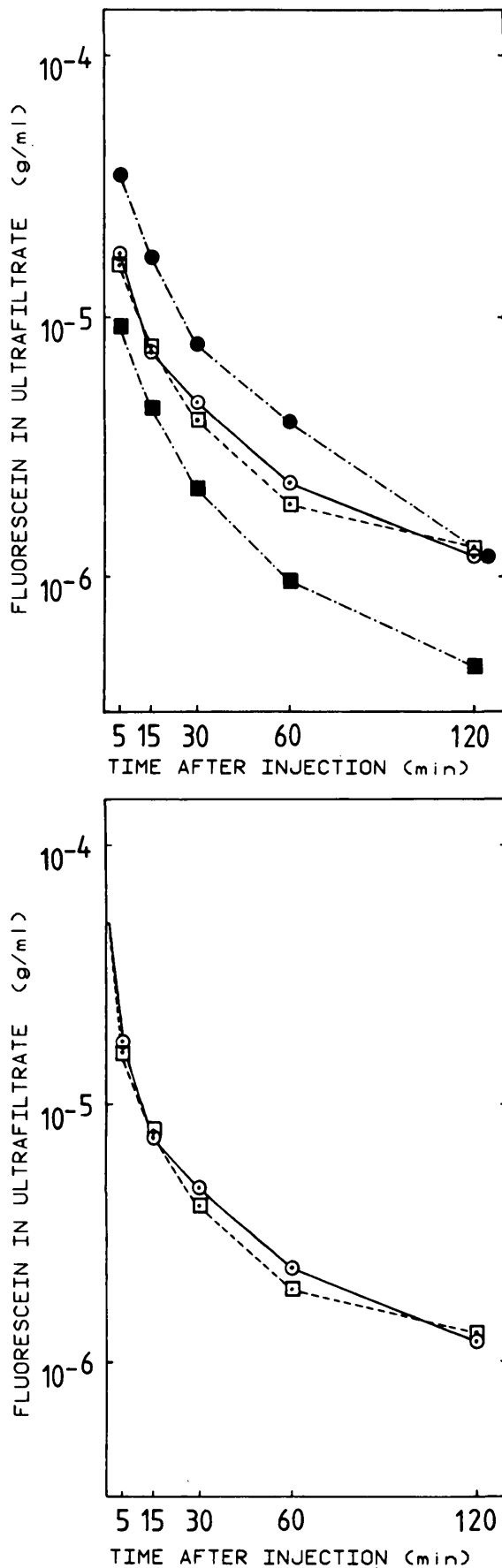
where $c_m(r_i, t)$ is the measured value at $r = r_i$, and c is the corresponding value given by equation (2).

Equation (5) indicates that each point of the vitreous concentration profile is weighted equally during the fitting procedure. In the paper by Larsen et al,¹⁰ another weighting procedure was suggested. However, this procedure adds too much weight to the low values towards the center of the eye and, accordingly, the present equal weighting procedure is preferred.

Results

Measurement of Fluorescein in Plasma and Eye

Figure 6A shows the plasma concentration time course of free non-protein-bound fluorescein in plasma



ultrafiltrate as it appears in a normal person and in a diabetic patient with background retinopathy.⁷ Together with these data, curves are also given representing those with the smallest and the largest area below the curve as obtained from 165 examinations. Figure 6B shows the plasma data for the normal person and the diabetic patient after linear extrapolation of the plasma fluorescein concentration from the 5-min value to the estimated concentration of 5×10^{-5} g/ml during the first minute of the injection (see Materials and Methods).

Fig. 7A shows an axial ocular concentration profile of fluorescein obtained 60 min after injection in the normal person and in the diabetic patient, respectively. Note the marker points indicating the positions of the slit-lamp focal plane in relation to the ocular structures.

It appears from the positions of the markers at point 1 (retina) and point 2 (vitreous body) that the peak of the signal is displaced towards vitreous from the position where the retina is in focus, both for a normal person and for a diabetic patient. This is a general phenomenon for all our readings. Similar results are reported by other authors.²¹ The position of the peak can be explained by the fact that the signal between points 1 and 2 is composed of the retinal fluorescence (choroid, retinal vasculature, and retinal cells) and the signal from fluorescein in the extracellular space of the retina, having passed the blood-retinal barrier. The mutual fluorescence of these components will determine the location of the peak. A higher fluorescein concentration in the extracellular space of the retina and vitreous will tend to draw the peak towards the vitreous, as also appears from Figure 7A. Due to the complexity of the signal between points 1 and 2, this part of the curve is not used for the calculations and only the curve from point 2 to the center of the eye is used, as described in detail elsewhere.¹⁰ It is assumed that the concentration of fluorescein is highest in the retinal extracellular space close to the barrier, but due to the complexity of the signal and the spatial integration in the optical diamond, this high concentration is not registered directly.

←
Fig. 6. A, *top*, Concentration of fluorescein in ultrafiltrate of plasma as a function of time from injection of fluorescein. Open circles represent a normal person. Open squares represent a diabetic patient. Closed circles represent the plasma fluorescein curve with the largest area under the curve, as obtained from 165 examinations, and closed squares represent the curve with the smallest area under the curve respectively. B, *bottom*, Extrapolation of plasma fluorescein values from 0 to 5 min (see Materials and Methods) for the normal person and the diabetic patient as shown in A. These curves are used for further calculations.

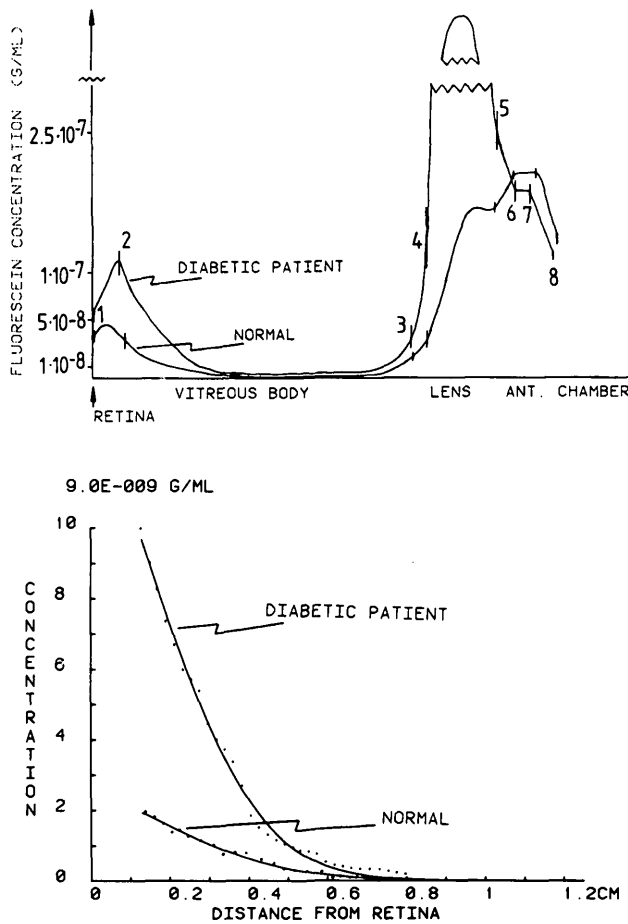


Fig. 7. A, top. Axial ocular concentration profile of fluorescein in a normal person and a diabetic patient with background retinopathy and macular edema 60 min after injection of fluorescein. The signal obtained corresponding to the lens represents autofluorescence of the lens. For the diabetic patient the lens signal was very large as illustrated by the interruption at the top. The numbered vertical bars are the marker points obtained according to the following system: point 1, retina in focus, with the blue slit in the middle of the optic fiber; point 2, optic fiber free of the blue slit-image on the retina (this position is located approximately 1.5 mm from the retina); point 3, optic fiber at the posterior lens surface; point 4, posterior lens surface in the middle of the optic fiber; point 5, anterior lens surface in the middle of the optic fiber; point 6, optic fiber at the anterior lens surface; point 7, optic fiber at the posterior corneal surface; point 8, posterior corneal surface in the middle of the optic fiber. B, bottom. The concentration profiles in the vitreous body as shown in A after reduction of data, subtraction of preinjection scan, and localization of the profile in the vitreous body. Only the part of the profile from marker point 2 to the center of the eye is used. Dots represent the directly observed concentration profile. This profile is together with the connected plasma curve (Fig. 6B) used for the computer calculations. The solid line represents the concentration profile calculated by the computer corresponding to the best fit of the model (Fig. 5) to the experimental data.

Figure 7B shows with dots the vitreous recordings from point 2 to the center of the eye after transformation to intraocular distance, correction for prein-

jection value, and reduction of data (see Materials and Methods). Connected plasma and vitreous data (Figs. 6B, 7B) are used for the calculation of the permeability and diffusion coefficient. The solid line represents the best fit of the model to the experimental data.

Calculation of P and D in Normals and in Patients with Diabetic Retinopathy

Table 1 gives the values of P and D for a group of normal persons, representing the low-permeation situation, and a group of diabetic patients with background retinopathy and macular edema, representing the high-permeation situation. It appears that the permeability is different for the two groups, whereas the diffusion coefficients are the same.

Calculation of P: In order to illustrate the effect on the magnitude of P of the various elements involved in its calculation, Table 2 shows P as calculated by the present method, by the present method with some modifications, and by another method. The results are calculated from data obtained 60 min after injection of fluorescein. The permeabilities for the normal person and the diabetic patient are shown on the left, and the diffusion coefficients are shown on the right. The effect of the various calculations is also given in percent in relation to the results obtained by the present method (first row). Correction for preinjection scan affects the low-permeation situation by 55%. Biologically reasonable variations of the bolus concentration affect the data approximately 25%, and application of a standard plasma curve instead of that determined for each individual person may lead to maximal errors between +39% and -47%. The

Table 1. Permeability (P) and diffusion coefficient (D) in a group of normal persons, representing the low permeation situation, and a similar group of diabetic patients with background retinopathy including macular edema, representing the high permeation situation*

| | Permeability (P) 1×10^{-7} cm/sec Mean (\pm SD) | Diffusion coefficient (D) 1×10^{-6} cm ² /sec Mean (\pm SD) |
|--|---|--|
| Normal persons | 1.1 (0.4) | 7.4 (3.4) |
| Background retinopathy including macular edema | 7.1 (3.8) | 9.6 (2.0) |

* The normal group was made up of 6 persons (2 women and 4 men) with mean age 32 yr, and the group of diabetic patients was made up of a similar group with mean age 32 yr, and an average duration of diabetes of 18 yr.

Table 2. Calculation of P and D for a normal person and a diabetic patient with background retinopathy including macular edema, representing the low permeability and the high permeability situation, respectively*

| | Permeability (P) 1×10^{-7} cm/sec | | | | Diffusion coefficient (D) 1×10^{-5} cm ² /sec | | | |
|--|--|-------------|------------------|-------------|---|-------------|------------------|-------------|
| | Normal person | | Diabetic patient | | Normal person | | Diabetic patient | |
| | P | Change in % | P | Change in % | D | Change in % | D | Change in % |
| Present calculation | 1.61 | — | 8.17 | — | 1.01 | — | 0.80 | — |
| No correction for preinjection value | 2.50 | +55 | 8.67 | +6 | 1.50 | +49 | 0.89 | +11 |
| Bolus not included | 1.92 | +19 | 10.10 | +24 | 1.06 | +6 | 0.85 | +6 |
| Bolus concentration (1×10^{-4} g/ml) | 1.22 | -24 | 6.14 | -25 | 0.95 | -6 | 0.74 | -8 |
| Application of highest plasma curve | 0.90 | -44 | 4.37 | -47 | 1.04 | +3 | 0.84 | +5 |
| Application of lowest plasma curve | 2.23 | +39 | 11.03 | +35 | 0.94 | -7 | 0.74 | -8 |
| Change in factor F (cf. Fig. 4) not included | 1.66 | +3 | 8.70 | +6 | 1.12 | +11 | 0.98 | +23 |
| P calculated as ratio between area under vitreous curve and plasma curve | 1.29 | -20 | 9.91 | +21 | — | — | — | — |

* Row 1 shows the values as they appear with the model calculation; row 2, the effect of the subtraction of the preinjection scan; row 3, the effect of the bolus on the calculation (with the plasma concentration assumed to be the same at time 0 as it is 5 min after injection); row 4, the effect of an increase of the bolus concentration to 1×10^{-4} g/ml; rows 5 and 6, the effect of the application in the calculations of the highest and lowest plasma concentration, respectively, obtained during 165 examinations; row 7, the effect of a correct

anatomical placement of the concentration profile in the vitreous body, and row 8, the value of P as it appears by a simple calculation as the ratio between area under vitreous fluorescein and plasma fluorescein curves. The values given in row 1 differ from those given in Table 1. This is due to the fact that data of Table 1 represent means of a group, whereas data of Table 2 represent a single person of the group.

other factors given in the table are of minor importance for P. For details see footnote to Table 2.

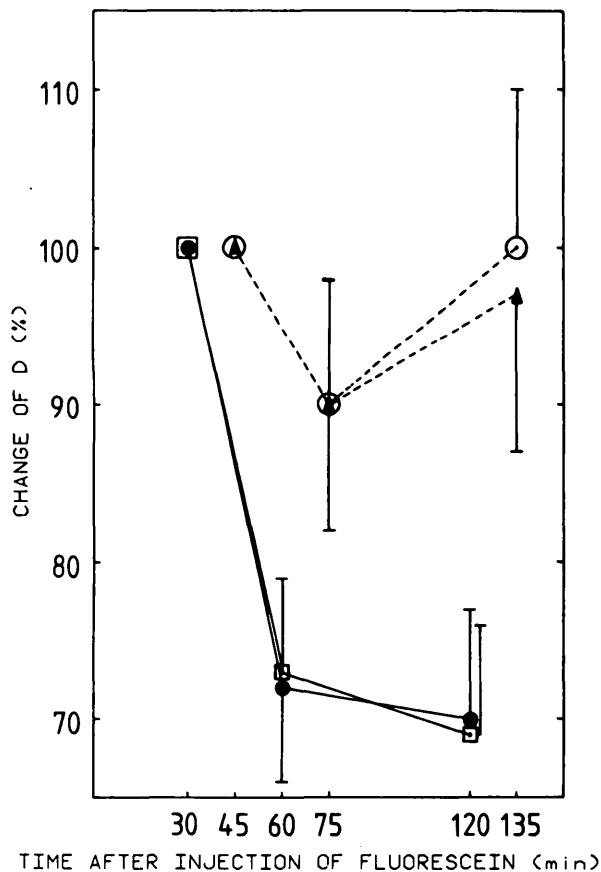
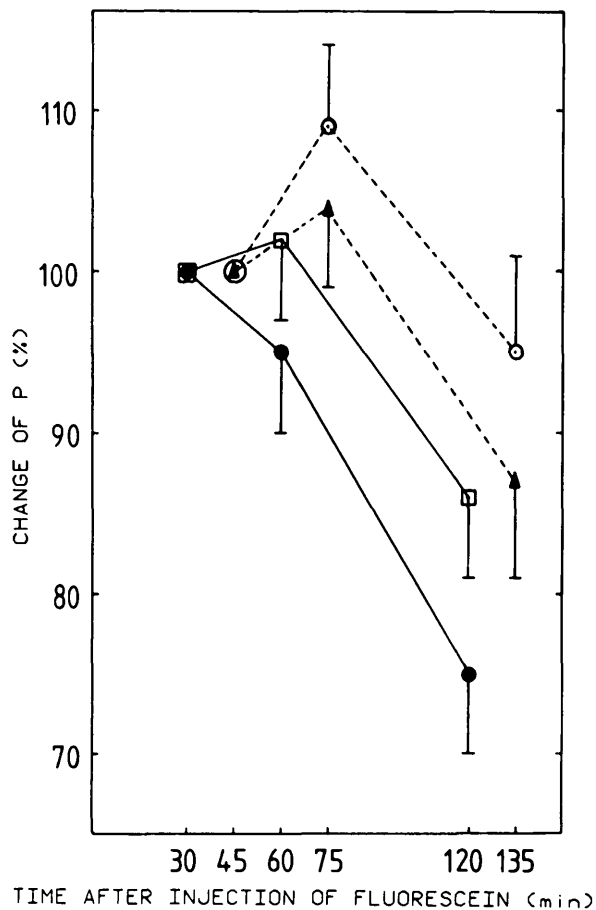
Calculation of D: The value of D is also shown in Table 2. The most important factor for the calculation of D is the correction for the preinjection value for the normal person and the incorporation of the factor F in the calculations for the diabetic patient. D is less sensitive to the variations, which are related to changes in plasma concentration.

Consistence of the Model as Evaluated as a Function of Time

The data reported so far were obtained by the application of the vitreous concentration profile obtained 60 min after fluorescein injection and the corresponding plasma curve from 0 to 60 min. However, the concentration profile in the vitreous body was routinely registered also 30 min and 120 min after fluorescein injection, and the plasma concentration was also followed over the 120-min period (Fig. 6). With the present method, P decreases 25% versus time as shown in Figure 8A (closed circles) where data representative of 69 diabetic patients with varying degrees of leakage are shown. P calculated after 30

min is arbitrarily given a value of 100%, and P calculated after 60 min and 120 min is expressed in relation to the 30-min value. The decrease of P versus time is only 15% when a bolus concentration of 1×10^{-4} g/ml is assumed, instead of 5×10^{-5} g/ml as it appears from the open squares. The decrease of P versus time is further diminished when it is taken into consideration that the concentration profile for methodologic reasons is obtained later than the blood samples are drawn. Assuming an interval of 15 min between blood sampling and slit-lamp determination (given by closed triangles), it appears that P varies only 10%. The same tendency for only a small variation of P versus time also appears when a bolus of 1×10^{-4} g/ml is assumed together with the 15-min separation between blood sampling and vitreous readings (open circles).

Figure 8B illustrates the effect of the same set of calculations on the magnitude of D. It appears that D decreases 30% versus time from 30 to 60 min and that this tendency is unaffected when a bolus of 1×10^{-4} g/ml is assumed. However, assuming the 15-min period between blood sampling and vitreous reading, D varies only 10% versus time. Unfortunately, the exact time of the registration of the vitreous



profile was not registered in the first 150 examinations, which is a methodologic shortcoming. After the temporal sensitivity of P and D were known, the exact time was registered and incorporated into the calculation formalism, which has led to only small variations of P and D versus time.

Discussion

The present article has mainly focused upon an introduction and evaluation of a slit-lamp fluorophotometric technique, which, by a combination of plasma and vitreous fluorescein concentrations, allows a calculation of a blood-retinal barrier permeability to fluorescein and a calculation of a diffusion coefficient for fluorescein in the vitreous body.

Equipment

The slit-lamp equipment is similar to that originally introduced by Cunha-Vaz and co-workers,¹ however, with some modifications and improvements. In order to optimize depth resolution a 100- μ m beam width and a 450- μ m probe diameter were applied.^{19,22} The sensitivity of the detection unit was improved by a factor of seven by the application of a chopped light system. Filters were improved by specially constructed interference filters, and movement of slit lamp was adjusted to the time constant of the detection unit by a servo acoustic mechanism. Special emphasis was given to a marking of the slit-lamp focal plane to perform a correct placement of the concentration profile in the vitreous body. Due to the spatial resolution of the slit lamp, the profile that was obtained 1.5 mm from the retina (point 2, Fig. 7A) was only insignificantly affected by the retinal and choroidal fluorescence. Accordingly, the part of the

←
Fig. 8. A, top, Permeability (P) and B, bottom, diffusion coefficient (D) versus time calculated by the model from corresponding values of plasma and vitreous fluorescein concentrations obtained 30, 60, and 120 min after injection of fluorescein. P and D obtained 30 min after injection are given a value of 100%, and P and D calculated from 60- and 120-min values are expressed relative (in %) to the 30-min value. The data are means of 10 diabetic patients representative of 69 patients with permeabilities from normal to 30 times normal. SEM is indicated by vertical bars. The values given by ●—● represent P and D as they appear by the calculation described in the methods and results. The value given by □—□ represents P and D as they appear if a bolus of 1×10^{-4} g/ml instead of 5×10^{-5} g/ml is used in the calculations (cf Fig. 6B). The value given by ▲—▲ represents P and D when the standard concentration in the bolus of 5×10^{-5} g/ml is used, but it is assumed that the concentration profile in the vitreous body is obtained 15 min later than the blood sampling. The value given by ○—○ represents P and D when a bolus of 1×10^{-4} g/ml and a 15-min period between blood sampling and vitreous readings is assumed.

curve between marker point 2 (Fig. 7A, 7B) and the center of the eye was used for the calculation, but the mathematical model automatically extrapolates from marker point 2 to the retina. The computer set-up made possible an automatic correction for preinjection scan, which is of special significance for the low-permeation situation.

Bolus

The present method of calculation applies the peripheral venous concentrations as representative for the fluorescein concentration on the blood side of the barrier. Application of the venous concentration instead of the capillary value is permissible for a substance like fluorescein, which has a very low extraction across the barrier. However, in the first minutes after injection, the peripheral venous concentration is not representative of the ocular venous concentration. Due to the net extraction in the peripheral capillaries (subject becomes yellow), the mixed peripheral venous concentration will be lower than the ocular. For a small water-soluble substance like fluorescein, with an expected capillary extraction of about 40%,²³ the net extraction will be minimal first after five circulation times, which is 3–4 min. Peripheral venous blood samples obtained earlier than 4 min after injection will thus underestimate the concentration at the barrier. Accordingly, we have chosen to estimate the ocular concentration in the bolus during the 1-min injection and to perform a simple linear extrapolation from the 1-min to the 5-min value. The present description and reasoning are based upon data and considerations, which are discussed in more detail elsewhere.^{23–25} The alternative method, in which the venous fluorescein concentration during the first minutes is used for the calculations, will maximally overestimate the value of P by 24% after 60 min (Table 2). The effect of the bolus is of larger significance when 30-min values are used for the calculations and also when a very rapid injection technique is used since the saturability of the fluorescein binding to plasma proteins will lead to a higher free (non-protein-bound) fluorescein concentration.^{5,6,26}

A bolus concentration of 5×10^{-5} g/ml is used for the calculations. Higher concentrations (maximally, 1×10^{-4} g/ml) may appear due to variations in stroke volume and due to the fact that the free fraction of 15%, as obtained in vitro, tends to increase during in vivo conditions.^{5,6,27}

Simplified Mathematical Model of the Eye

The model is a considerable simplification of the biologic system. However, the simplification seems to be permissible, as will appear from the following

reasoning. The blood-retinal barrier is symbolized by a single membrane, even though it is anatomically composed of two membrane systems. However, due to the short anatomic distance between the two structures compared with the slow movement of fluorescein through the vitreous, these two barriers cannot be separated, and a single membrane formalism symbolizing both barriers is permissible. The vitreous body is compared with a homogeneous gel in which fluorescein moves only by diffusion.²⁸ The model is symmetric, not taking the anatomic asymmetry of the eye in consideration. However, because the model is applied to situations in which the contribution of fluorescein from the anterior segment is only minimal (Fig. 7), the symmetric model assumption is permissible.

It also appears that P is assumed to be equal in both directions, despite the fact that it has been suggested that selective active transport of fluorescein occurs in the direction from the vitreous body to blood in animals²⁹ and in humans.^{3,9} However, these suggestions are based upon examinations in which transport across the anterior blood vitreous barrier (epithelium of ciliary body) cannot be distinguished from transport across the blood-retinal barrier. Accordingly, we have chosen the simplest model without active transport, since it is able to account for the experimental data. That this is a reasonable assumption will appear from the following reasoning.

Constancy of P and D versus time supports the simple model assumption. However, as shown in Figures 8A, B, there was a tendency towards a decrease of P and D versus time within the first 2 hr of examination. This might be a consequence of active transport that was not incorporated into the model. However, this tendency was only small when the concentration of fluorescein in the bolus was assumed to be 1×10^{-4} g/ml instead of 5×10^{-5} g/ml, and it was taken into consideration that due to practical circumstances some minutes (maximally, 15 min) elapsed between blood sampling and vitreous readings. It appears that reasonable variations of the two parameters involved in the model calculations lead to a stability of both P and D versus time, thus, not supporting an active transport mechanism across the blood-retinal barrier. Furthermore, preliminary calculations where an active transport process across the blood-retinal barrier from vitreous to blood is introduced does not lead to a better correlation between model and experimental data. Thus, there seems to be substantial experimental evidence for the simplified model of the eye, without active transport across the blood-retinal barrier as far as it is applied in short time situations in which the anterior part of the eye does not affect the transient state of fluid and

solute exchange in the posterior part of the eye. This conclusion is also supported by recent studies by Zeimer et al.^{13,30}

The permeability P: P is defined as the permeability factor, which in the model formalism combines the concentration of fluorescein in plasma and vitreous body [equations (2) and (3)]. Thus, P reflects all kinds of transport processes, both passive transport according to the electrochemical gradient and possible active transport occurring along and against the electrochemical gradient. In the model, P is a real permeability constant (cm/sec). However, when the model P is interpreted in terms of permeability of the biologic barrier, it has to be correlated to the area of the biologic barrier. This area is unknown and is composed of two different epithelial systems. In order to obtain an impression of the maximal magnitude of the permeability of the biologic barrier (Pb) for comparison with other data, Pb can be estimated according to the following reasoning:

P is connected with Pb according to the following equation:

$$Pb \times Sb = P \times S \text{ (cm}^3\text{/sec)} \quad (6)$$

where Sb and S represent the surface area of the biological barriers and the model, respectively. Assuming a radius of the eye of 1.2 cm and that retina constitutes two thirds of the sphere, it follows from equation (6) that

$$Pb \times Sb = 12P \text{ (cm}^3\text{/sec)}. \quad (7)$$

Since Sb is not known, it is convenient to express the permeability of the biologic barrier as $Pb \times Sb$, in accordance with the PS product known from capillary physiology.³¹ Sb can be evaluated according to the following reasoning. Assuming that the central retinal artery system is comparable to the cerebral circulation, Sb from that system is 240 cm²/g.³² The weight of the retina is 0.25 g. The smallest possible area of the pigment epithelium (not taking foldings of cell membranes into account) is two thirds of the area of the sphere (≈ 12 cm²). Accordingly, $Sb \approx 72$ cm², and from equation (7) it follows that

$$Pb = 1.6P \times 10^{-1} \text{ (cm/sec)}. \quad (8)$$

For a normal person with $P = 1.1 \times 10^{-7}$ cm/sec, $Pb = 1.8 \times 10^{-8}$ cm/sec, which is 10 times lower than the maximal K⁺ permeability estimated in rat brain capillaries³³ and even lower than that estimated for K⁺ in frog brain microvasculature.³⁴ A similar calculation shows that Pb for a diabetic patient is 1.1×10^{-7} cm/sec. It also follows from equation (6) that an increase of the area of the biological barrier by the model will be mimicked by an increase in P and vice versa for a decrease in biologic area.

Also, changes in electrical potential can lead to changes of the magnitude of P without reflecting permeability changes for other uncharged molecules.

Variation of P due to method: It appeared from Table 2 that P varied according to the various procedures used for its calculation. The most important factor for the calculation was that originating from variations in the concentration of fluorescein in plasma, which accounted for a factor of 30–50%. This fact stresses the importance of a plasma fluorescein determination and incorporation of the plasma data in the calculation if measurements with an accuracy greater than $\pm 50\%$ are required. Also the concentration of fluorescein in the bolus plays a role as discussed earlier. For the low-permeation situation, the subtraction of the preinjection scan is also of considerable significance. The other factors mentioned in Table 2 only affect the value of P within 20%. Calculated as the ratio between area under vitreous curve and plasma curve,³⁵ P differs only within 20% from that calculated by the model.

Two previously published papers employ a permeability constant that is calculated by a combination of plasma and vitreous fluorescence signals using a mathematical model.^{3,13} Palestine and Brubaker³ derived a retinal permeability of $1.5\text{--}2.5 \times 10^{-6}$ cm/sec. Their elegant measurements, however, were performed with an unsatisfactory axial resolution and in a position in the anterior part of the vitreous body, where the blood-aqueous barrier may influence the data significantly. Recently, Zeimer et al¹³ have refined the model and used it in a pharmacokinetic interpretation of vitreous fluorophotometry in the posterior part of the vitreous body. The value of P in their normal group was 1.2×10^{-7} cm/sec, in very good agreement with that given in this article, even though the assumptions and the mathematical model of the two papers are somewhat different. This concordance mutually confirms the validity of both even though Zeimer et al¹³ have to use a higher vitreous diffusion coefficient in order to derive the same permeability factor as reported in this article.

The diffusion coefficient: The movement of fluorescein through the vitreous body is quantitated by a diffusion coefficient. The diffusion coefficient which is found with the present method corresponds approximately to free diffusion in water.²⁹ The quantitation of the diffusion coefficient is sensitive to the exact placement of the concentration profile in the vitreous body. A diffusion coefficient of the same magnitude has been indirectly found by Palestine and Brubaker³ for the anterior part of the vitreous body. However, it is difficult to compare the diffusion coefficients due to the differences in methodology. Zeimer et al¹³ derive a higher diffusion coefficient in

normal persons than found in this article. This difference may be explained by the fact that the position of the concentration profile in the vitreous body plays a significant role for the magnitude of *D* (Table 2). A formalism which does not take the exact positioning into account will tend to give higher *D* values than those obtained in this article.

General Comments to the Method

The present technique is introduced in an attempt to increase the reproducibility and accuracy of the vitreous fluorophotometric method. The present model formalism allows a quantitation of a permeability and diffusion coefficient, which is, per se, of importance, and which can be used as a tool in a quantitative evaluation of ocular barrier and vitreous relationships. Three factors are not directly elucidated by the model. One factor is the effect of the absorption of light occurring in the lens. In a recent study by Zeimer et al,³⁰ this factor has been evaluated and may be of significance, especially for older persons. No satisfactory quantitative solution of this problem is available at present. Another problem is the metabolism of fluorescein. The fluorescence signal thus reflects both fluorescein and its glucuronide in the plasma water phase. However, with the present filter combination and IV administration of fluorescein, the photometric interference between fluorescein and glucuronidated fluorescein is less than 10% at 60 min after injection.³⁶⁻³⁸ Thus, the fluorescence signal is interpreted in terms of free—non-protein bound—fluorescein alone. However, even if the photometric interference is only of minor significance, interference between the two substances may occur at the transport sites of the blood-retinal barrier; therefore, the relation between unbound fluorescein and glucuronidated fluorescein has to be evaluated in more detail. The third factor is transport phenomena across the anterior barrier system, which is important for examinations longer than 2 hr in duration and for the high permeation situation, in which the contribution of fluorescein from the anterior segment of the eye is important within the 2-hr period. This is the subject of a model elaboration which is in preparation at present.

Key words: vitreous fluorophotometry, blood-retinal barrier permeability, vitreous body diffusion coefficient, fluorescein

References

- Cunha-Vaz JG, Abreu JF, Campos AJ, and Figo GM: Early breakdown of the blood-retinal barrier in diabetes. *Br J Ophthalmol* 59:649, 1975.
- Cunha-Vaz JG: The blood-ocular barriers. *Surv Ophthalmol* 23:279, 1979.
- Palestine AG and Brubaker RF: Pharmacokinetics of fluorescein in the vitreous. *Invest Ophthalmol Vis Sci* 21:542, 1981.
- Lund-Andersen H and Lassen NA: Microvascular permeability in diabetic patients. *Bibl Anat* 20:675, 1981.
- Brubaker RF, Penniston JT, Grotte DA, and Nagataki S: Measurement of fluorescein binding in human plasma using fluorescence polarization. *Arch Ophthalmol* 100:625, 1982.
- Lund-Andersen H and Krogsaa B: Fluorescein in human plasma in vitro. *Acta Ophthalmol* 60:701, 1982.
- Lund-Andersen H, Krogsaa B, and Jensen PK: Fluorescein in human plasma in vivo. *Acta Ophthalmol* 60:709, 1982.
- Palestine AG and Brubaker RF: Plasma binding of fluorescein in normal subjects and in diabetic patients. *Arch Ophthalmol* 100:1160, 1982.
- Blair NP, Zeimer RC, Rusin MM, and Cunha-Vaz JG: Outward transport of fluorescein from the vitreous in normal human subjects. *Arch Ophthalmol* 101:1117, 1983.
- Larsen J, Lund-Andersen H, and Krogsaa B: Transient transport across the blood-retinal barrier. *Bull Math Biol* 45:749, 1983.
- Lund-Andersen H, Krogsaa B, and Larsen J: Computerized calculation of the blood-retinal barrier permeability and vitreous body diffusion coefficient for fluorescein in man. *ACTA: XXIV International Congress of Ophthalmology*, Henkind P, editor. London, JB Lippincott, 1983, pp. 458-462.
- Lund-Andersen H, Krogsaa B, and Larsen J: The calculation of the blood-retinal barrier permeability to fluorescein. *Proceedings of the International Symposium on Ocular Fluorophotometry*, Paris, 1982. *Grafe's Arch Clin Exp Ophthalmol* 1985, in press.
- Zeimer RC, Blair NP, and Cunha-Vaz JG: Pharmacokinetic interpretation of vitreous fluorophotometry. *Invest Ophthalmol Vis Sci* 24:1374, 1983.
- Prager TC, Chu H-H, Garcia CA, and Anderson RE: The influence of vitreous change on vitreous fluorophotometry. *Arch Ophthalmol* 100:594, 1982.
- Krogsaa B, Fledelius H, Larsen J, and Lund-Andersen H: Photometric oculometry: a slit lamp technique for determination of intraocular distances. *Proceedings of the International Symposium on Ocular Fluorophotometry*, Paris, 1982. *Grafe's Arch Clin Exp Ophthalmol* 1985, in press.
- Lund-Andersen H, Krogsaa B, Larsen J, Scherfig E, and Sesstoft L: A fluorophotometric evaluation of the functional state of the vitreous body in the development of diabetic retinopathy. *Proceedings from the International Symposium on Retinal Diseases*, Ryan S, editor, San Diego, 1982, in press.
- Krogsaa B, Fledelius H, Larsen J, and Lund-Andersen H: Photometric oculometry. I. An analysis of the optical principles in slit lamp fluorophotometry. *Acta Ophthalmol* 62:274, 1984.
- Bursell S-E, Delori FC, and Yoshida A: Instrument characterization for vitreous fluorophotometry. *Curr Eye Res* 1:711, 1982.
- Zeimer RC, Cunha-Vaz JG, and Johnson ME: Studies on the technique of vitreous fluorophotometry. *Invest Ophthalmol Vis Sci* 22:668, 1982.
- Krogsaa B, Fledelius H, Larsen J, and Lund-Andersen H: Photometric oculometry. II. Measurement of axial ocular distances with slit lamp microscopy: clinical evaluation and comparison with ultrasonography. *Acta Ophthalmol* 62:290, 1984.
- Bursell S-E, Delori FC, Yoshida A, Parker JS, Collas GD, and McMeel JW: Vitreous fluorophotometric evaluation of diabetics. *Invest Ophthalmol Vis Sci* 25:703, 1984.
- Prager TC, Wilson DJ, Avery GD, Merritt JH, Garcia CA, Hopen G, and Anderson RE: Vitreous fluorophotometry:

- identification of sources of variability. *Invest Ophthalmol Vis Sci* 21:854, 1981.
23. Guyton AC: Textbook of Medical Physiology, Table 30-1. Philadelphia, WB Saunders, 1976, p. 389.
 24. Alm A: Microcirculation of the eye. *In* The Physiology and Pharmacology of the Microcirculation, Mortillaro NA, editor. New York, Academic Press, 1983, pp. 299-359.
 25. Lund-Andersen H: Transport of glucose from blood to brain. *Physiol Rev* 59:305, 1979.
 26. Li W and Rockey H: Fluorescein binding to normal human serum proteins demonstrated by equilibrium dialysis. *Arch Ophthalmol* 100:484, 1982.
 27. Penniston JT: Fluorescence polarization measurement of binding of fluorescein to albumin. *Exp Eye Res* 34:435, 1982.
 28. Fatt I: The vitreous body. *In* Physiology of the Eye, Fatt I, editor. Woburn, Butterworths, 1978, pp. 77-83.
 29. Cunha-Vaz JG and Maurice DM: The active transport of fluorescein by the retinal vessels and the retina. *J Physiol* 191: 467, 1967.
 30. Zeimer RC, Blair NP, and Cunha-Vaz JG: Vitreous fluorophotometry for clinical research. *Arch Ophthalmol* 101:1757, 1983.
 31. Crone C: Capillary permeability: techniques and problems. *In* Capillary Permeability: The Transfer of Molecules and Ions between Capillary Blood and Tissue, Crone C and Lassen NA, editors. Copenhagen, Munksgaard, 1970, pp. 15-31.
 32. Crone C: The permeability of capillaries in various organs as determined by use of the "indicator diffusion" method. *Acta Physiol Scand* 58:292, 1963.
 33. Hansen AJ, Lund-Andersen H, and Crone C: K⁺ permeability of the blood-brain barrier investigated by aid of a K⁺ sensitive microelectrode. *Acta Physiol Scand* 101:438, 1977.
 34. Crone C and Olsen SP: Electrical resistance of brain microvascular endothelium. *Brain Res* 241:49, 1982.
 35. Krogsaa B, Lund-Andersen H, Mehlsen H, Sestoft L, and Larsen J: The blood-retinal barrier permeability in diabetic retinopathy. *Acta Ophthalmol* 59:689, 1981.
 36. Arie M, Sawa M, Nagataki S, and Mishima S: Aqueous humor dynamics in man as studied by oral fluorescein. *Jpn J Ophthalmol* 24:346, 1980.
 37. Chen S-C, Nakamura H, and Tamura Z: Studies on the metabolites of fluorescein in rabbit and human urine. *Chem Pharm Bull (Tokyo)* 28:1403, 1980.
 38. Chen S-C, Nakamura H, and Tamura Z: Determination of fluorescein and fluorescein monoglucuronide excreted in urine. *Chem Pharm Bull (Tokyo)* 28:2812, 1980.